Four Verification Cases for PORODRY

We designed four different verification cases to validate different aspects of our numerical solution and its code implementation, and these are summarized in Table 1.

Table 1. Summary of Verification Cases

Verification Case #	General Description
1	Slit flow; $Re = 1000$
2	Backward-step flow; $Re = 805$
3	Advection of Gaussian (bell-shaped) solute concentration profile in flow; $Pe = 1$, $Pe = 100$
4	Drying of a 21×21 pore-network with one side open to the constant environment vapor concentration $C_{\infty} = 0$.

Verification 1 is a 2-D incompressible laminar slit-flow, where there is a theoretical result available for comparison. Verification 2 is a 2-D backward-step flow, and the results are compared with a previous experiment and simulation (Lee, 1998). These two cases are chosen to verify our N-S equations solver for the outside flow-field, which is the first step of our proposed algorithm. Verification 3 is to simulate a transient 1-D species advection problem such that the results are compared with a theoretical solution (Muralidhar, et al., 1993). This is used to test the accuracy of the solver for solving the transportation equation which includes convection and diffusion. Verification 4 uses the results of a previous pore-network model (Shaeri, 2012) to examine our I-P algorithm implementation and thus establish the accuracy of our P-N simulation.

1 SLIT FLOW

Verification 1 is using a 2-D incompressible laminar flow in a slit between two parallel plates to test the N-S solver with its Hayase QUICK scheme and SIMPLER algorithm. To simulate a fully-developed slit flow, the periodic boundary conditions are set on the inlet and outlet sides of the tunnel, and the inlet side is given a higher pressure while the outlet side is given a lower pressure. No-slip wall boundary conditions are applied on the top and bottom sides, as shown in Figure 1.

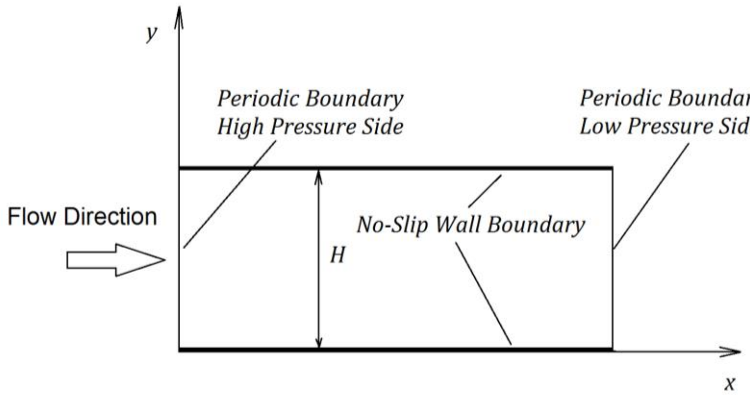

Figure 1. A schematic describing the geometry and boundary conditions of the considered 2-D slit flow

In this verification, the distance between slits $H = 0.1\ m$; the tunnel length is set equal to H; pressure difference between the inlet and outlet is $0.0003276\ Pa$; the fluid is air with its density as $\rho_{air} = 1.204\ kg/m^3$, and dynamic viscosity as $\mu_{air} = 1.813 \times 10^{-5}\ Pa \cdot S$.

The analytical solution to this problem is:

$$\mathrm{u(y)} = \left(-\frac{dp}{dx}\right)\frac{H^2}{8\mu}[1 - (\frac{y}{H/_2})^2] \tag{1}$$

According to equation (1), the peak velocity for this case is $0.2259\ m/s$ while the average velocity is $U_{avg} = 0.1506\ m/s$. As expected, the peak velocity is 1.5 times the average velocity. The Reynolds Number $Re = \rho_{air}U_{avg}H/\mu_{air} = 1000$.

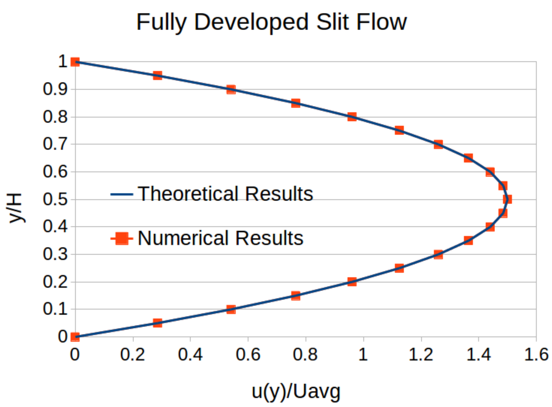

Figure 2. Velocity Profile Comparison between Theoretical and Numerical Results

The comparison between the numerical and theoretical results is presented in dimensionless form in Figure 2. The numerical results agree perfectly with the analytical results, thus establishing the accuracy of our numerical solution for steady-state laminar flow in 2-D.

2 BACKWARD-STEP FLOW

Verification 2 is using a 2-D incompressible laminar flow in backward-step geometry, as shown in Figure 3, to test the N-S solver with its hybrid scheme and SIMPLE algorithm.

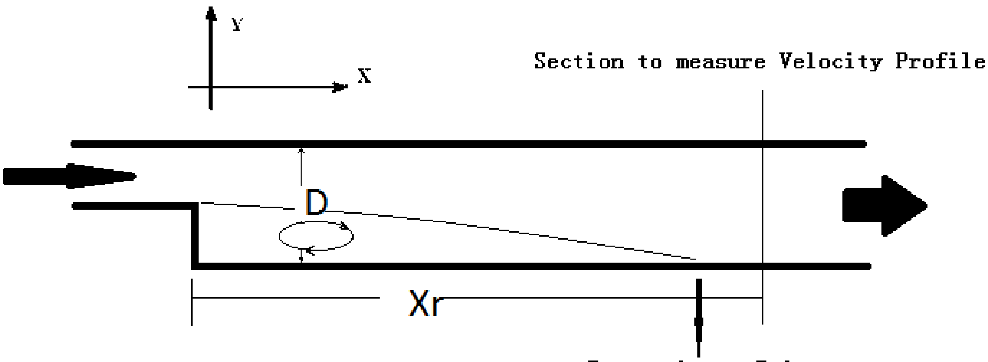

Figure 3. A schematic of the backward-step flow geometry

The backward step geometry is chosen, because it is widely studied through experiments and numerical simulations. By doing this verification, we can examine the ability of our implementation to capture the detachment of channel flow at the back of the step and subsequent re-attachment.

As shown in Figure 3, the tunnel height after the step, D, is $0.03\ m$; the tunnel height before the step is $D/2$. The tunnel walls have no-slip wall boundary conditions. The flow's inlet average velocity is $U_{avg} = 0.4041\ m/s$ and the fluid is air just the same as that in Section 3.1. So the Reynolds number $Re = \rho_{air} U_{avg} D/\mu_{air} = 805$. To make the results comparable to the experiment and simulation by (Lee & Mateescu, 1998), the inlet velocity is not uniform—instead it is assigned the fully-developed velocity distribution calculated from equation (1).

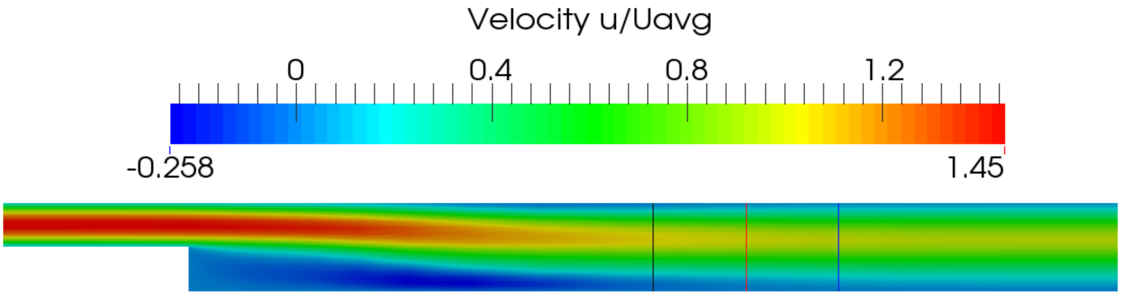

Figure 4. Velocity contour for the backward-step flow

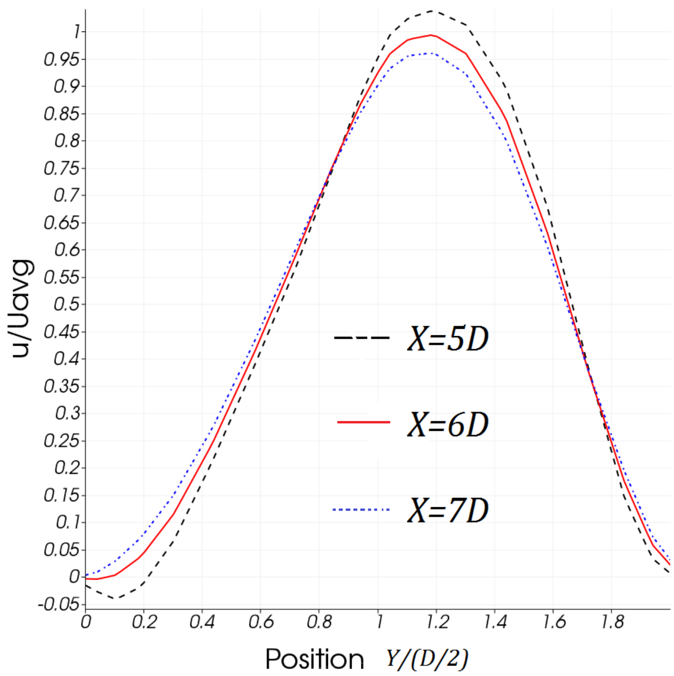

Figure 5. Numerically obtained backward-step flow velocity profiles at different cross-sections

Figure 4 shows the velocity contour of our numerical simulation. Note that there are three cross sections after the step; their locations are $x = 5D$, $x = 6D$, $x = 7D$, and they are marked respectively as black, red and blue lines. Their colors correspond with the colors used in Figure 5, which shows the velocity profiles at the said cross sections.

In Figure 5, the lower left corner at $Y = 0$ is the velocity near the lower wall of the tunnel. We observe that the velocity turns from negative to positive right between section $x = 6D$ and $x = 7D$, which implies that the reattachment point is located between these two sections. This result is almost identical to the numerical results presented by Lee & Mateescu and is only a little off from their experimental result of $7D$. This means our numerical implementation of the outside flow involving complex flow-circulation and flow-reattachment physics is quite accurate, and it allows us to believe that our external-flow simulation can handle much more complex flow geometries than currently used in verification case 1 and 2.

3 ADVECTION OF A GAUSSIAN CONCENTRATION DISTRIBUTION

Verification 3 uses a 1-D salute transport problem with analytical solution to compare with the results from our code to examine the accuracy of the operator-splitting solver of the transportation equations. This is a 1-D advection problem along the x axis as shown in Figure 6. We set an initial Gaussian or bell-shaped concentration distribution on the left side of the 1-D domain. As time goes by, the Gaussian distribution will dissipate and will be pushed to the right due to fluid flow from the left side.

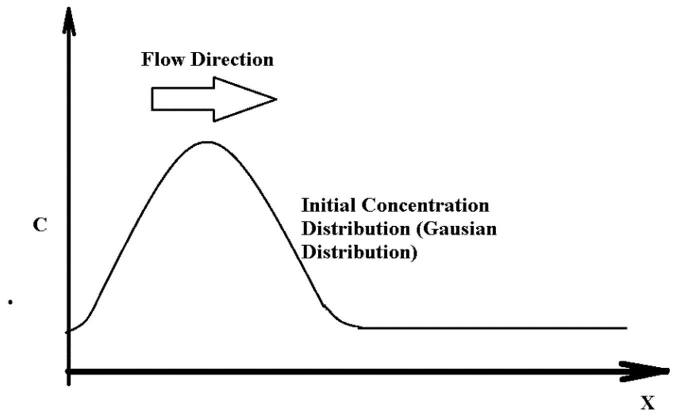

Figure 6. Schematic description of the code verification carried out by using the advection of Gaussian concentration distribution

The results of this problem can be calculated by numerically solving the convection diffusion transportation equation. Its theoretical solution (Muralidhar, et al., 1993) is given as: If the Initial distribution is described as

$$t = 0,\ C(x,\ 0) = e^{-\alpha(x-x_0)^2} \tag{2}$$

in which α is a constant parameter for controlling the width of the bell-shaped curve and the x_0 is a constant locating the center of the curve. The analytical solution to this problem is given as

$$\begin{gathered} C(x,t) = \frac{1}{2}\sqrt{\frac{Pe}{\pi t}}e^{\left(\frac{x}{2}-\frac{t}{4}\right)Pe}\int_0^x F(x,\ y,\ t)dy \\ F(x,\ y,t) = e^{-\alpha(y-x_0)^2-\frac{yPe}{2}} \times [e^{-(x-y)^2\frac{Pe}{4t}} - e^{-(x+y)^2\frac{Pe}{4t}}] \end{gathered} \tag{3}$$

Figure 7 compares the analytical solution, equation (3), with the numerical results obtained from solving the transportation equations for two different Peclet number values. We observe that at the higher Pe with advection dominant, the curves seem to be translating downstream with the flow. However, at lower Pe with diffusion dominant, the curves seem to be rooted on the left side and seem to be merely stretching with time. But both sets of curves show a decay in the maximum height with time, the lower Pe being more so. But it is heartening to note that the numerical results match perfectly with the analytical solutions for the considered high and low *Pe* cases.

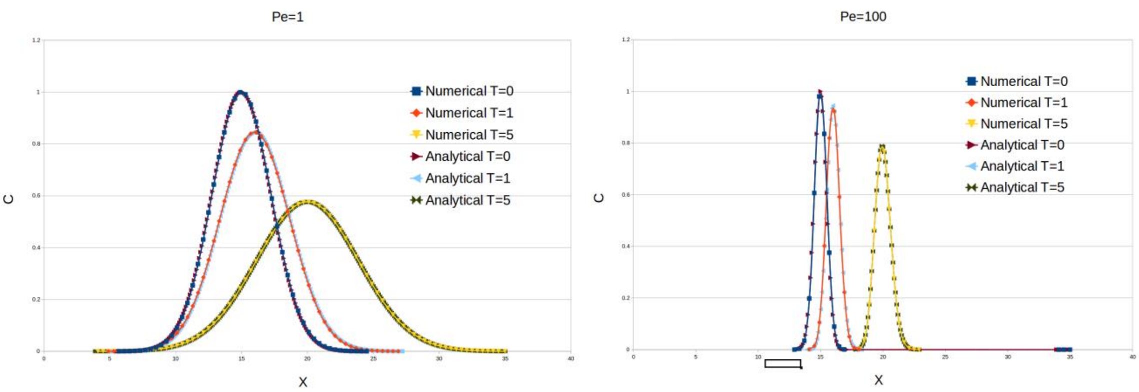

Figure 7. Advection of Gausian concentration distribution (Left $Pe = 1$, right $Pe = 100$): a comparison of the numerical solution with the analytical solution

4 VERIFICATION OF THE I-P ALGORITHM BASED NETWORK DRYING MODULE

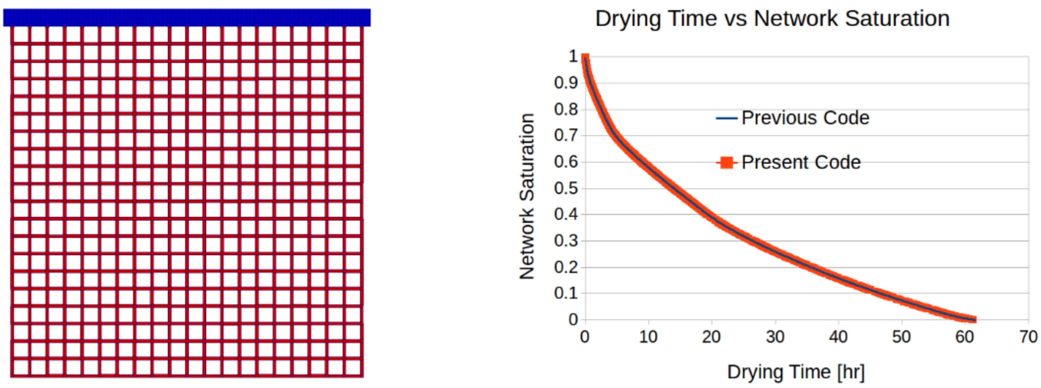

Figure 8. Verification of drying physics implementation (Left: calculation domain; Right: drying time-vs-network saturation plot)

To validate our I-P algorithm based numerical code for simulating drying inside the pore-network, we compared our results with the results obtained by our previous, independently-developed code (Shaeri, 2012).

This is a 21×21 network with one side open to the environment of constant species (water vapor) concentration set equal to 0, as shown in Figure 8. The left side shows that initially the network is filled with liquid, colored as red; and the environment concentration is set as a constant of 0, colored as blue. The right side plots the drying time-vs-network saturation. The network saturation is defined as the ratio of the liquid mass present currently in the network versus the liquid mass corresponding to the fully-saturated network. The results from the present code match perfectly with the results obtained from the previous code, thereby established the accuracy of our numerical implementation of the I-P algorithm.

Reference

Bear, J., 1988. *Dynamics of Fluids in Porous Media.* s.l.:Dover Publications.

Beyhaghi, S., Xu, Z. & Pillai, K. M., n.d. Achieving the inside-outside Coupling during Simulation of Isothermal Drying of a Porous Medium in a Turbulent Flow. *Transport in*

Porous Media (Under Review).

Freitas, D. S. & Prat, M., 2000. Pore Network Simulation of Evaporation of a Binary Liquid from a Capillary Porous Medium. *Transport in Porous Media,* Volume 40, pp. 1-25.

Huinink, H. P. & Pei, L., 2002. Drying Processes in the Presence of Temperature Gradients-Pore-Scale Modeling. *European Physical Journal E,* Volume 9, pp. 487-498.

Laurindo, J. B. & Prat, M., 1996. Numerical and Experimental Network Study of Evaporation in Capillary Porous Media-Phase Distributions. *Chemical Engineering Science,* 51(23), pp. 5171-5185.

Laurindo, J. B. & Prat, M., 1998. Numerical and Experimental Network Study of Evaporation in Capillary Porous Media-Drying Rates. *Chemical Engineering Science,* 53(12), pp. 2257-2269.

Lee, T. & Mateescu, D., 1998. Experimental and Numerical Investigation of 2-D Backward-Facing Step Flow. *Journal of Fluids and Structures,* Volume 12, pp. 703-716.

Metzger, T., Irawan, A. & Tsotsas, E., 2007. Isothermal Drying of Pore Networks: Influence of Friction for Different Pore Structures. *Drying Technology,* Volume 25, pp. 49-57.

Metzger, T. & Tsostas, E., 2008. Viscous Stabilitization of Drying Front: Three-Dimensional Pore Network Simulations. *Chemical Engineering Research and Design,* Volume 86, pp. 739-744.

Muralidhar, K., Verghese, M. & Pillai, K. M., 1993. Application of an Operator-Splitting Algorithm for Advection-Diffusion Problems. *Numerical Heat Transfer Part A,* Volume 23, pp. 99-113.

Nowicki, S. C. & Davis, H. T., 1992. Microscopic Determination of Transport Parameters in Drying Porous Media. *Drying Technology,* 10(4), pp. 925-946.

Patankar, S. V., 1980. *Numerical Heat Transfer and Fluid Flow.* s.l.:Taylor & Francis.

Pillai, K. M., Prat, M. & Marcoux, M., 2009. A Study on Slow Evaporation of Liquids in a Dual-Porosity Porous Medium using Square Network Model. *International Jorunal of Heat and Mass Transfer,* Volume 52, pp. 1643-1656.

Plourde, F. & Prat, M., 2003. Pore Network Simulations of Drying of Capillary Porous Media. Influence of Thermal Gradients. *International Jorunal of Heat and Mass Transfer,* Volume 46, pp. 1293-1307.

Prat, M., 1993. Percolation Model of Drying under Isothermal Conditions in Porous Media. *International Journal of Multiphase Flow,* 19(4), pp. 691-704.

Prat, M., 2007. On the Influence of Pore Shape, Contact Angle and Film Flows on Drying of Capillary Porous Media. *International Journal of Heat and Mass Transfer,* Volume 50, pp. 1455-1468.

Prat, M., 2011. *Heat and Mass Transfer in Capillary Structures-Application to Loop Heat Pipes.* Minsk, VIII International Seminar.

Quintard, M. & Whitaker, S., 1993. Transport in ordered and disordered porous media: volume-averaged equations, closure problems, and comparison with experiment. *Chemical Engineering Science,* 48(14), pp. 2537-2564.

Shaeri, M. R., 2012. *Investigating Regular Pore-Network Models to Predict Drying in Porous Media,* Milwaukee: s.n.

Shaeri, M. R., Beyhaghi, S. & Pillai, K. M., 2012. Drying of a Porous Mediu, with Multiple Open Sides using a Pore-Network Model Simulation. *International Communications in Heat and Mass Transfer,* 39(9), pp. 1320-1324.

Shaeri, M. R., Beyhaghi, S. & Pillai, K. M., 2013. On Applying an External-Flow Driven Mass Transfer Boundary Condition to Simulate Drying from a Pore-Network Model. *International Journal of Heat and Mass Transfer,* Volume 57, pp. 331-344.

Surasani, V. K. & Metzger, T., 2006. *Towards a Complete Pore Network Drying Model: First Steps to Include Heat Transfer.* Gifu, 15th International Drying Symposium.

Tsilingiris, P., 2008. Thermophysical and transport properties of humid air at temperature range between 0 and 100 C. *Energy Conversion and Management,* Volume 49, pp. 1098-1110.

Versteeg, H. K. & Malalasekera, W., 2007. *An Introduction to Computational Fluid Dynamics - The Finite Volume Method.* 2 ed. s.l.:Pearson.

White, F. M., 1999. *Fluid Mechanics.* 4 ed. s.l.:McGraw-Hill.

Yiotis, A. G. B. A. G., Stubos, A. K., Tsimpanogiannis, I. N. & Yortsos, Y. C., 2004. Effect of liquid films on the drying of porous media. *AIChE Journal,* Volume 50, pp. 2721-2737.

Yiotis, A. G. & Boudouvis, A. G., 2003. Effect of Liquid Films on the Isothermal Drying of Porous Media. *Physical Review E,* Volume 68, p. 037303.

Yiotis, A. G. & Stubos, A. K., 2001. A 2-D Pore-Network Model of the Drying of Single-Component Liquids in Porous Media. *Advances in Water Resources,* Volume 24, pp. 439-460.

Yiotis, A. G. & Stubos, A. K., 2005. Pore-Network Modeling of Isothermal Drying in Porous

Media,. *Transport in Porous Media,* Volume 58, pp. 63-86.

Yiotis, A. G. & Tsimpanogiannis, I. N., 2006. Pore-Network Study of the Characteristic Periods in the Drying of Porous Materials. *Journal of Colloid and Interface Science,* Volume 297, pp. 738-748.

Yiotis, A. G. & Tsimpanogiannis, I. N., 2007. Coupling between external and internal mass transfer drying of a porous medium. *Water Resource Research,* 43(6), p. W06403.

YioZalesak, S. T., 1979. Fully Multidimensional Flux-Corrected Transport Algorithms for Fluids,. *Journal of Computational Physics,* Volume 31, pp. 335-362.

Zhou, D., Blunt, M. & Orr, F. M. J., 1997. Hydrocarbon Drainage along Corners of Noncircular Capillaries. *Journal of Colloid and Interface Science,* Volume 187, pp. 11-21.